






## Article

# Design and Optimization of Microbial Fuel Cells and Evaluation of a New Air-Breathing Cathode Based on Carbon Felt Modified with a Hydrogel—Ion Jelly<sup>®</sup>

Rui N. L. Carvalho <sup>1</sup>, Luisa L. Monteiro <sup>1</sup> , Silvia A. Sousa <sup>1</sup> , Sudarsu V. Ramanaiah <sup>2</sup>, Jorge H. Leitão <sup>3</sup> , Cristina M. Cordas <sup>4</sup>  and Luis P. Fonseca <sup>3,\*</sup> 

- <sup>1</sup> Institute for Bioengineering and Biosciences (iBB), Instituto Superior Técnico (IST), Universidade de Lisboa (UL), Av. Rovisco Pais, 1049-001 Lisboa, Portugal; ruicarlov@gmail.com (R.N.L.C.); luis4lopesmonteiro@gmail.com (L.L.M.); sousasilvia@tecnico.ulisboa.pt (S.A.S.)
- <sup>2</sup> Food and Biotechnology Research Lab, South Ural State University (National Research University), 454080 Chelyabinsk, Russia; ramanasudarsan@gmail.com
- <sup>3</sup> Department of Bioengineering (DBE), Institute for Bioengineering and Biosciences (iBB), The Associate Laboratory Institute for Health and Bioeconomy (i4HB), Instituto Superior Técnico (IST), Universidade de Lisboa (UL), Avenida Rovisco Pais, 1049-001 Lisboa, Portugal; jorgeleitao@tecnico.ulisboa.pt
- <sup>4</sup> Associated Laboratory for Green Chemistry of the Network of Chemistry and Technology (LAQV-REQUIMTE), Department of Chemistry, NOVA School of Science and Technology, Universidade Nova de Lisboa, 2829-516 Caparica, Portugal; c.cordas@fct.unl.pt
- \* Correspondence: luis.fonseca@tecnico.ulisboa.pt; Tel.: +351-218419139

**Abstract:** The increased demand for alternative sustainable energy sources has boosted research in the field of fuel cells (FC). Among these, microbial fuel cells (MFC), based on microbial anodes and different types of cathodes, have been the subject of renewed interest due to their ability to simultaneously perform wastewater treatment and bioelectricity generation. Several different MFCs have been proposed in this work using different conditions and configurations, namely cathode materials, membranes, external resistances, and microbial composition, among other factors. This work reports the design and optimization of MFC performance and evaluates a hydrogel (Ion Jelly<sup>®</sup>) modified air-breathing cathode, with and without an immobilized laccase enzyme. This MFC configuration was also compared with other MFC configuration performances, namely abiotic and biocathodes, concerning wastewater treatment and electricity generation. Similar efficiencies in COD reduction, voltage (375 mV), PD (48 mW/m<sup>2</sup>), CD (130 mA/m<sup>2</sup>), and OCP (534 mV) were obtained. The results point out the important role of Ion Jelly<sup>®</sup> in improving the MFC air-breathing cathode performance as it has the advantage that its electroconductivity properties can be designed before modifying the cathode electrodes. The biofilm on MFC anodic electrodes presented a lower microbial diversity than the wastewater treatment effluent used as inocula, and inclusively Geobacteracea was also identified due to the high microbial selective niches constituted by MFC systems.

**Keywords:** microbial fuel cells; bioelectricity; air-breathing cathode; Ion Jelly<sup>®</sup>, laccases; wastewater treatment



**Citation:** Carvalho, R.N.L.; Monteiro, L.L.; Sousa, S.A.; Ramanaiah, S.V.; Leitão, J.H.; Cordas, C.M.; Fonseca, L.P. Design and Optimization of Microbial Fuel Cells and Evaluation of a New Air-Breathing Cathode Based on Carbon Felt Modified with a Hydrogel—Ion Jelly<sup>®</sup>. *Energies* **2023**, *16*, 4238. <https://doi.org/10.3390/en16104238>

Academic Editors: Alexandra M.F.R. Pinto and Vânia Sofia Brochado de Oliveira

Received: 27 April 2023

Revised: 17 May 2023

Accepted: 18 May 2023

Published: 22 May 2023



**Copyright:** © 2023 by the authors. Licensee MDPI, Basel, Switzerland. This article is an open access article distributed under the terms and conditions of the Creative Commons Attribution (CC BY) license (<https://creativecommons.org/licenses/by/4.0/>).

## 1. Introduction

The electricity produced worldwide comes traditionally from coal, gas, oil, and nuclear energy due to easy access to these resources. However, these traditional energy sources are associated with a wide range of environmental problems and are limited by their scarcity. Consequently, today the search for renewable energy production with fewer or zero carbon emissions to the atmosphere and environmental impact emerges. Renewable energy sources are of fundamental importance for the sustainability of actual and future human generations, as stated in the UN 2030 Agenda for Sustainable Development [1]. Renewable energy sources include solar photovoltaics, farm and onshore wind, water movement in

tides and waves, geothermal heat, biomass conversion, and others often deployed with further electricity generation. These renewable energies and deploying energy efficiency technologies result in significant energy security, climate change mitigation, and economic benefits (net zero carbon emissions).

Fuel cells, particularly microbial fuel cells, are characterized like other renewable energy sources to generate clean electric energy, for example, consumed locally by wastewater treatment plants and rural (off-grid) energy services. Among the renewable energy sources, the advantage of the MFCs is that they simultaneously reduce organic compound content in domestic and industrial effluents responsible for environmental problems and pollution.

Conventional effluent treatments based on aerobic biological reactors can efficiently degrade and reduce the content of those organic pollutants but without energy production. Additionally, the requirements for aeration and sludge generation, among other factors, make these operations expensive [2]. Other methods such as anaerobic digestion produce methane in the form of biogas while dark fermentation produces hydrogen and can be used as fuels converted into electric energy. In contrast, the MFCs produce bioelectricity without needing any other energy conversion process, i.e., converting fuel into electricity.

In recent years, fuel cells (FC) have been progressively developed and are considered a possible solution to energy sustainability supply as they are electrochemical devices capable of converting chemical compounds into electrical energy with good efficiency and low emissions [3]. Among FC are the microbial fuel cells (MFCs), where the anolyte (and in some cases, also the catholyte) comprise consortia of microorganisms. The primary importance of applying MFCs is the possibility of using microbial systems to degrade and reduce the COD content of wastewater effluents of industrial and domestic origin and simultaneously generate electrical energy [4].

The MFCs consist of bioelectrochemical systems in which a bioreactor is used in different configurations, being the most common the one with two independent chambers, the anodic and cathodic compartments [5]. The microorganisms that inoculate the anodic compartment of MFCs should include exoelectrogenic bacteria. These bacteria have a high capacity to generate electrons, protons, and other metabolic products resulting from the metabolization of organic matter [6]. The electrons generated are transferred to the anodic electrode either by electron mediators (e.g., neutral red, anthraquinone derivative [7]) or the microorganisms (mediator-less) by direct membrane-associated electron transfer, nanowires, and others [8,9].

The generated protons are transported to the cathodic chamber through the proton exchange membrane, while electrons are transferred externally to the cathode electrode with simultaneous electricity production. The protons and electrons that achieve the cathode electrode react with oxygen, producing water [10].

The current generation rate cannot exceed the rate at which exoelectrogenic bacteria release electrons to the anode electrode surface. Usually, the current generation is limited by the diffusion of organic matter due to a biofilm grown on the anodic electrode surface and mainly when a thicker or impenetrable biofilm occurs [11]. Another limitation is associated with the balance activity of electrogenic versus methanogenic microbes on the anode electrode surface, as the last one is not responsible for generating electrical energy but only for reducing COD. A shift in these microbial populations on the electrode surface can occur during a long-term period of operation using a natural biological source for MFC inoculation, such as collected from wastewater treatment effluents [12].

The MFC performance should maximize COD removal efficiency and electricity production, while the oxygen should be fully available at the cathode compartment as an electron acceptor. Mateo et al. [13] observed that the current density and COD removal in wastewater effluent treatment drastically falls when working at lower oxygen concentrations because of increased limitations of oxygen mass transfer in the cathodic compartment. The low oxygen solubility in aqueous effluents implies that the cathodic reaction can become the limiting stage of the MFC performance [14]. The conventional MFC setup

uses dissolved oxygen cathodes bubbling air continuously in the cathodic compartment to minimize oxygen limitations, but the costly aeration can limit its full-scale application [15].

Palmore et al. [16] reported a biocathode with laccase and 2,2'-azino-bis(3-ethylbenzothiazoline-6-sulfonic acid (ABTS) in solution characterized by lower activation overpotentials than using a platinum electrode and resulting in increased performance on the oxygen reduction in the cathode. One drawback of using laccase in solution is that only limited oxygen concentrations are present. Furthermore, laccases are sensitive to deactivation in the presence of chloride ions [17], and electroactive species commonly found in biological systems, such as ascorbic acid, can compete with oxygen reduction. Usually, interference of these compounds can be mitigated using a protective layer of ionic liquid (1-butyl-3-methylimidazolium hexafluorophosphate) [18], and one way to solve the low oxygen concentration would be to eliminate the cathodic solution.

Recently, significant interest has been focused on designing and developing MFC air-breathing cathodes with great potential to overcome the limitations mentioned above and to continue contributing to wastewater and other effluents treatment and simultaneous electricity generation [19–23].

Air-breathing cathodes are used in traditional hydrogen fuel and have also been used in some previously reported MFCs for wastewater treatment [13,24,25]. Additionally, redox enzymes have been tested on the catalytic process and direct transfer of electrons to reduce oxygen on the cathode electrode. The most recent evolution of this research was to combine the advantages of these cathodes with multicopper oxidases, such as laccase, creating biocathodes that use oxygen directly from atmospheric air [26–28]. However, there are still problems employing enzymes for air-breathing cathodes because enzymes need to remain hydrated, and most enzyme reactions occur in solution and not in the gas phase [29].

Air-breathing cathodes containing laccase have already been tested in some biofuel cells with enzymatic anodes [30,31] or a pure-culture microbial anode, where a power density (PD) of 211 mW/m<sup>2</sup> was obtained [32].

Ion Jelly<sup>®</sup> (hydrogel based on ionic liquids and gelatin), previously developed by the authors, is a conductive, transparent, and flexible polymer material that combines the chemical versatility of organic salt–ionic liquid (IL) with the morphological versatility of a natural and inexpensive biopolymer—gelatin [33,34]. This compound is biocompatible, targets thin-film batteries, and has good ionic conductivity (10<sup>−4</sup> S/cm) and a wide electrochemical window, and presents high stability at 180 °C, establishing stable hydrogen bonds between the IL and ionic gelatin.

Ion Jelly<sup>®</sup> was tested in this work to stabilize laccase using a methodology similar to that previously used to stabilize oxidoreductase enzymes (e.g., glucose oxidase, peroxidase) [35]. The MFC air-breathing cathodes with or without immobilized laccase in Ion Jelly materials were tested for oxygen reduction directly from the air.

Previous work carried out by our research group led to the design of MFCs with a microbial community from a wastewater treatment plant oxidizing a synthetic fuel and reducing oxygen using microbial biocathode or abiotic cathodes. In this work, the influence of the materials used on the MFC setup configuration, such as carbon felt used as electrodes, copper wires, a Nafion membrane, external resistance in the electric circuit between electrodes, and the effect of agitation in the anodic chamber for the wastewater treatment, was initially tested.

Based on those optimized design MFC configurations, a new MFC air-breathing cathode was developed for effluent treatment and bioelectricity generation and compared with previous work using MFC abiotic cathode and biocathode configurations [36].

Finally, the microbial composition of biomass collected from a wastewater treatment plant, used to inoculate the MFC systems, and samples from biofilm formed on the anode electrode surfaces were analyzed.

## 2. Materials and Methods

### 2.1. MFC Design

MFC is constituted by two poly(methyl methacrylate) compartments in “H” design, with a liquid volume of 360 mL each with a lateral opening (6 cm × 6 cm) plus 3 other small orifices for discharge, feeding, and sampling (Figure 1A).

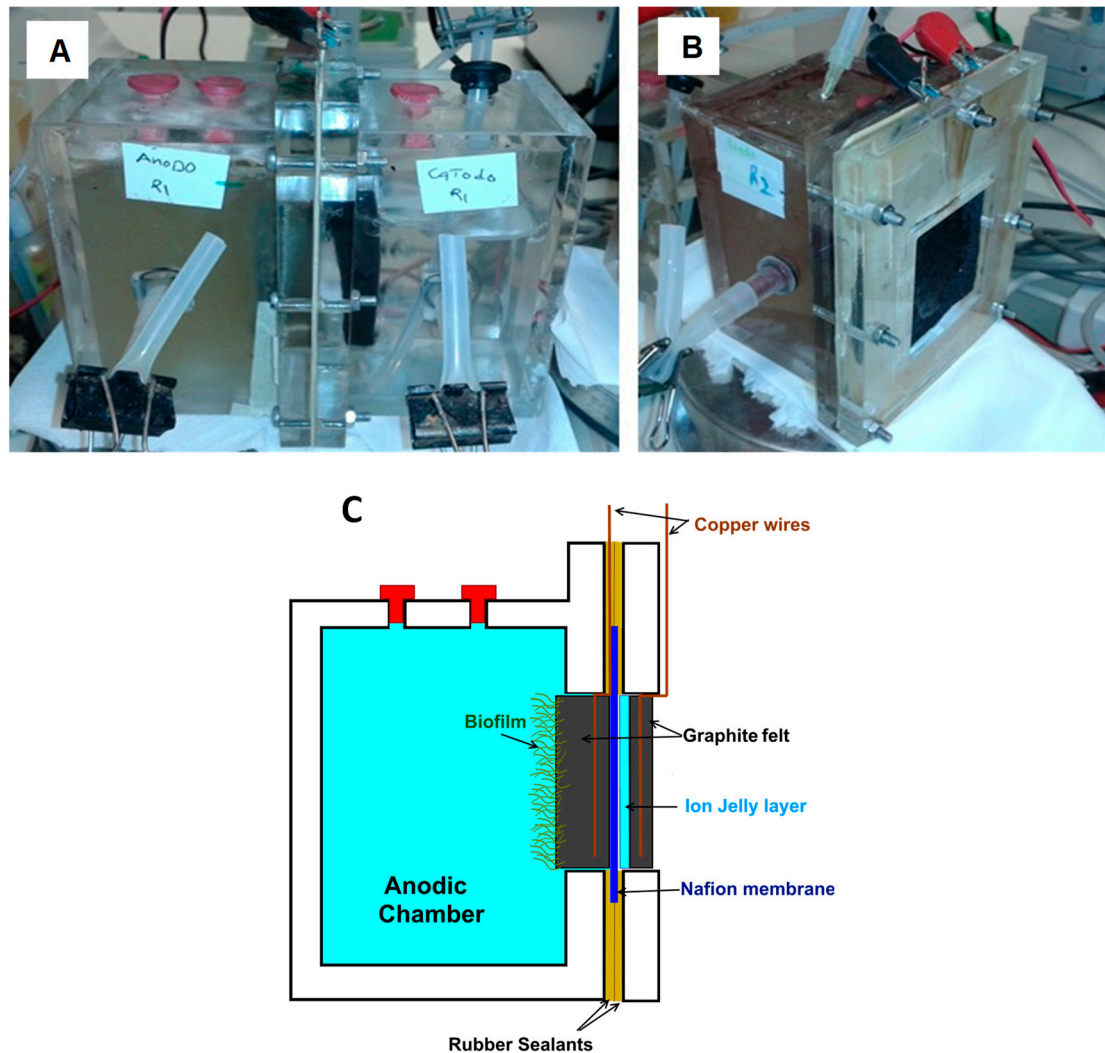


**Figure 1.** MFC setup. (A) MFC H-form separated by a Nafion membrane. (B) MFC with an anode chamber and carbon felt cathode in direct contact with air. (C) Schematic cross-section of an assembled MFC with an air-breathing cathode.

A 3 mm thick rubber gasket was used on both sides of the compartments to prevent leakage. A 0.18 mm thick Nafion membrane (Alfa Aesar, A Johnson Matthey Company, Ward Hill, MA, USA) (7 cm × 7 cm) separated both chambers, allowing selective proton exchange ( $H^+$ ) between the chambers and preventing oxygen in the anodic chamber. The Nafion N-117 membrane was previously hydrated in distilled water for 12 h to enhance its elasticity. The electrode material in both chambers was based on a 5 mm thick carbon felt (Alfa Aesar, A Johnson Matthey Company), with a copper wire connecting each electrode for external current collection.

The copper wires integrated into both electrodes were connected to an external resistance and a digital multimeter system (Keithley Integra 2700/7700, Cleveland, OH, USA) for data acquisition (at least every 5 min) of the operating voltage to monitor electrical

energy generation and MFC performance, and exporting the experimental data to a desktop computer.

During the experiments, the anode compartment was under anaerobic conditions by bubbling N<sub>2</sub> for 30 min in an aqueous solution (360 mL) based on a synthetic wastewater effluent and inoculum of microorganisms consortium (biomass inoculum) collected from a wastewater treatment plant (Chelas, Lisbon City, Portugal).

The abiotic cathode had the usual configuration of the cathode compartment, initially containing phosphate buffer (50 mM, pH 7, 360 mL). Air was bubbled continuously using a small air compressor (ELITE mark—801 C Holf Nagen, UK. Ltd., Castleford, UK) to maintain aerobic conditions and O<sub>2</sub> as the electron and H<sup>+</sup> acceptor. Potassium permanganate, an oxidizing agent at a concentration of 0.4 mM, was also added to the phosphate buffer and tested to enhance the MFC abiotic cathode performance.

An MFC biocathode configuration was tested by loading sodium carbonate (3 mM) in phosphate buffer (50 mM, pH 7) and inoculating the cathode compartment with biomass inoculum.

The performance of MFC air-breathing cathodes with the carbon felt electrode in direct contact with air (Figure 1B) was also tested using the carbon felt without any modification and modified with an Ion Jelly solution according to the schematic cross-section presented in Figure 1C.

Optimization studies and evaluation of the different types of cathodes were operated in the batch operation mode at room temperature (≈22–25 °C). When the potential difference between both compartments was about 0 mV, a value representing the end of a batch cycle with almost total carbon source consumption, the batch operation was interrupted. The biomass was left to deposit for 20 min, and the exhausted effluent was discharged, leaving a residual volume of about 25% of the total liquid volume (i.e., about 90 mL). New synthetic wastewater effluent (270 mL) was added to initiate a new cycle.

Samples were collected from MFC compartments at the beginning and end of each cycle for subsequent chemical analysis.

## 2.2. Description of the Synthetic Wastewater Effluent

Most MFC research studies have concentrated on maximizing bioelectricity generation instead of COD removal efficiency, and few use single carbon sources from synthetic or natural wastewater effluents [37,38].

In this work, the MFC anodic and cathodic compartments were fed with synthetic wastewater effluent and buffers, respectively, with specific chemical compositions and volumes depending on the cathode types tested (Table 1).

**Table 1.** Chemical composition of synthetic wastewater effluent and buffers used in the MFC anode and cathode compartments.

Chemical Compounds	Anode	Biocathode	Abiotic Cathode
Sodium acetate (g/L)	0.82	-	-
Dihydrogen phosphate (g/L)	5.75	5.75	5.75
Dipotassium phosphate (g/L)	10.04	10.04	10.04
Ammonium chloride (g/L)	1.06	-	-
Sodium carbonate (g/L)	-	1.05	-
H <sub>2</sub> O (distilled water) (mL)	270	270	360
Inoculum 25% (mL)	90	90	-

The synthetic wastewater effluent was optimized and evaluated previously to meet the metabolic needs of this microorganism consortium and to be able to produce electrical energy [36]. The pH of the aqueous solutions in both compartments was kept almost constant at pH 7 using the phosphate buffer.



### 2.3. Description of the Inoculum

The microbial consortium used as biomass inoculum was collected from the entrance to the secondary settlement tank of a wastewater treatment plant (Chelas, Lisbon city, Portugal) and contained low organic matter content.

### 2.4. Microbial Consortium Composition and Concentration of Collected Samples

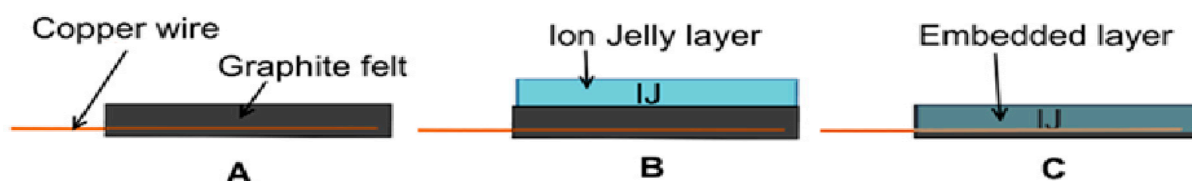
DNA extraction, sequencing, and data analysis of the microbial consortium composition were performed by DNA Sense (Aalborg, Denmark), and the methodology used is described in detail in the Supplementary Materials.

A total of ten samples were analyzed for microbial population composition and identification. Six biofilm samples were collected from the carbon felt surface of MFC anodic reactors (numbered 5 to 10), two samples were from the domestic wastewater treatment plant (numbered 3 and 4) and used as inoculum of the MFCs, and two samples were used as control collected from a different wastewater treatment plant stream (samples 1 and 2) (Supplementary Materials Table S1, also include references between [39–48]).

### 2.5. Design Conditions and Optimization of MFC Assembling Performance

When the MFC assembly guaranteed the absence of water leakage, the synthetic wastewater effluent or buffers were added into the respective compartments. The design conditions and optimization of MFC assembling performance were initially designed and organized in sequential experimental steps identified by numerical design condition (Condition #). The design condition experiments follow:

- Condition 1, the anodic and cathodic chambers contained 360 mL of synthetic wastewater effluent and phosphate buffer, respectively. The copper wires were initially immersed in each chamber, contacted with a resistance of 1000  $\Omega$  integrated into the external electric circuit to analyze interference and spontaneous oxidation of chemical compounds present in the synthetic wastewater effluent.
- Condition 2, the copper wires were attached inside the carbon felt (Scheme 1, configuration A) at a distance of  $\approx 10$  cm from each other, i.e., each electrode was maintained at a distance of  $\approx 5$  cm from the Nafion membrane.
- Condition 3, the anodic compartment operating without agitation was renewed with 270 mL of synthetic wastewater effluent, and then 90 mL of biomass inoculum was initially added. The anode compartment was sparkled with nitrogen gas for 30 min to replace the dissolved oxygen ( $O_2$ ) to achieve an anaerobic environment.
- Condition 4, each electrode distance to the Nafion membrane was reduced to  $\approx 2.5$  cm, checking if it influenced the generation of electric current by this MFC configuration.
- Condition 5, the carbon felt electrodes were pressed against the Nafion membrane, and they were at a distance from each other of about 0.5 cm, i.e., the thickness of the Nafion membrane. The synthetic effluent was renewed, and the anodic compartment continued operating without agitation for two new sequential cycles by feeding the synthetic wastewater effluent.
- Condition 6, the polarization effect was studied by varying the external resistance from 20 to 5000  $\Omega$  integrated into the external electric circuit between the anode and cathode electrodes.
- Condition 7, the anodic compartment was operated under magnetic agitation in the bottom to guarantee the homogenization of liquid content.



**Scheme 1.** Scheme of the different air-breathing cathode configurations tested. (A) Copper wire attached to graphite also named carbon felt; (B) Deposition of Ion Jelly layer on the top side of the carbon felt surface; (C) Carbon felt embedded with Ion Jelly.

### 2.6. Synthesis of Ion Jelly<sup>®</sup> and Preparation of Air-Breathing Cathodes

Ion Jelly<sup>®</sup> (IJ) was prepared as follows: 1.0 mL of 1-butyl-3-methylimidazolium dicyanamide [bmim][N(CN)<sub>2</sub>] provided by IoLiTec (Heibronn, Germany) was mixed with 0.8 g gelatin (Sigma-Aldrich, Lisbon, Portugal) at 40 °C. Then, 2.6 mL of citrate–phosphate buffer solution was added (buffer A, 50 mM pH 4). The IL solution was then stirred for an additional 10 min before modification of carbon felt.

The IJ solution covered one side of the dry carbon felt surface, forming a thin layer (Scheme 1, configuration B). A second strategy used a wetted carbon felt, previously immersed in water for 24 h, and then the IJ embedded in the wetted carbon felt. In this case, the IJ solution was previously mixed with *Trametes versicolor* laccase ( $\geq 0.5$  U/mg) from Sigma-Aldrich dissolved in 1.3 mL of buffer A. Sixty milligrams of laccase substituted the same amount of gelatin in the IJ solution preparation, corresponding to about 2.5 mg/cm<sup>2</sup> of the projected area of carbon felt (Scheme 1, configuration C).

In all cases, the modified carbon felt electrodes were allowed to cool at room conditions for an hour before a maturation step at controlled water activity and temperature conditions for at least 4 days (4 °C, water activity  $a_w$  of 0.76) [49].

### 2.7. Cyclic Voltammetry Analysis

Cyclic voltammetry (CV) was also used to identify reduction and oxidation reactions promoted by the redox-active compounds in the synthetic wastewater effluent at room temperature using a potentiostat (CHI Instruments 440B Electrochemical Analyzer, USA). The CVs were carried out inside a Faraday cage at a 50 mV/s scan rate. The MFC's anode and cathode were the working and counter electrodes, respectively, and a silver/silver chloride (Ag/AgCl) was the reference electrode.

### 2.8. Determination of Bioenergy Generation and MFC Performance

The current intensity ( $I$ ) expressed in Ampere (A) was calculated by Ohm's law (Equation (1)):

$$I = \frac{V_{MFC}}{R_{ext}} \quad (1)$$

$R_{ext}$  is the external electrical resistance system ( $\Omega$ ),  $V_{MFC}$  is the electric potential difference of the MFC in volts (V), and  $I$  is the intensity of electric current in ampere (A).

The MFC system power ( $P$ ) is expressed in W and calculated using Equation (2):

$$P = V_{MFC} * I \quad (2)$$

The current density (CD) expressed in A/m<sup>2</sup> was determined using Equation (3):

$$CD = \frac{I}{A_{anode}} \quad (3)$$

$A_{anode}$  corresponds to the projected surface area of the anode (m<sup>2</sup>) and  $I$  the current intensity (A).

The power density ( $PD$ ) expressed in  $W/m^2$  was calculated by power versus projected surface area of the anode ( $A_{\text{anode}}$ ) (Equation (4)):

$$PD = \frac{P}{A_{\text{anode}}} \quad (4)$$

The maximum power ( $P_{\text{max}}$ ) depends on the internal resistance system ( $R_{\text{int}}$ ). Therefore, their potency is low if an MFC has high internal resistance. The maximum power generated is related to the open circuit voltage (OCV) and calculated according to Equation (5):

$$P_{\text{max}} = \frac{OCV^2 * R_{\text{ext}}}{(R_{\text{int}} + R_{\text{ext}})^2} \quad (5)$$

The coulombic efficiency ( $CE$ ), expressed in percentage (%), is defined as the ratio between the number of coulombs effectively transferred to the anode and the total number of Coulombs produced, considering that all oxidized substrates produce electrons (Equation (6)).

$$CE = \frac{M * I}{F * b * q * COD} \quad (6)$$

$M$  is the molecular oxygen mass (32 g/mol),  $I$  the current intensity,  $F$  is the Faraday constant,  $b$  is the number of electrons transferred per mole of oxygen ( $4e^-$ ),  $q$  is the flow rate (L/s), and  $COD$  is the chemical oxygen demand ( $gO_2/L$ ).

### 2.9. Determination of COD by Potassium Dichromate Method

The COD was determined using the standard potassium dichromate digestion method [50]. Samples were centrifuged at 4000 rpm for 10 min or filtered with a 0.1  $\mu\text{m}$  Millipore PVDF membrane filter to remove microorganisms. To 1.5 mL of the sample, 1 mL of  $K_2Cr_2O_7$  digestion solution and 2 mL of  $AgSO_4$  solution (10 g/L in  $H_2SO_4$ ) were added. The mixture was digested at 150 °C for 2 h in a Labnet Accublock Digital Dry Bath (USA). The excess dichromate was titrated with a 12.5 mM ferrous ammonium sulfate solution (FAS). The volume (mL) of FAS necessary to titrate the sample (A) and a blank made with water (B) were noted down, and COD was calculated through the following expression (Equation (7)):

$$COD (mgO_2/L) = \frac{(A - B) * [FAS] * 8000}{V_{\text{sample}}} \quad (7)$$

[FAS] is the molarity of FAS solution (12.5 mM) and  $V_{\text{sample}}$  of the sample volume (1.5 mL).

## 3. Results and Discussions

### 3.1. Design Conditions and Optimization of MFC Assembly Performance

Design conditions were initially planned to detect the influence of the materials and operation mode during the construction and optimization of the MFC assembly. The bioenergy generation was measured for the different design conditions, particularly the placement of carbon felt with the copper wires, their distance to the Nafion membrane, and the addition of the synthetic wastewater effluent and biomass inoculum (Figure 2).

The first 10 days of analysis of MFC performance reveals that the materials used, such as copper wires alone (Condition 1) and carbon felt electrodes with copper wire at 5 cm from Nafion membrane (Condition 2), did not generate electrical energy, and they do not promote spontaneous oxidation of chemical compounds in the synthetic wastewater effluent.



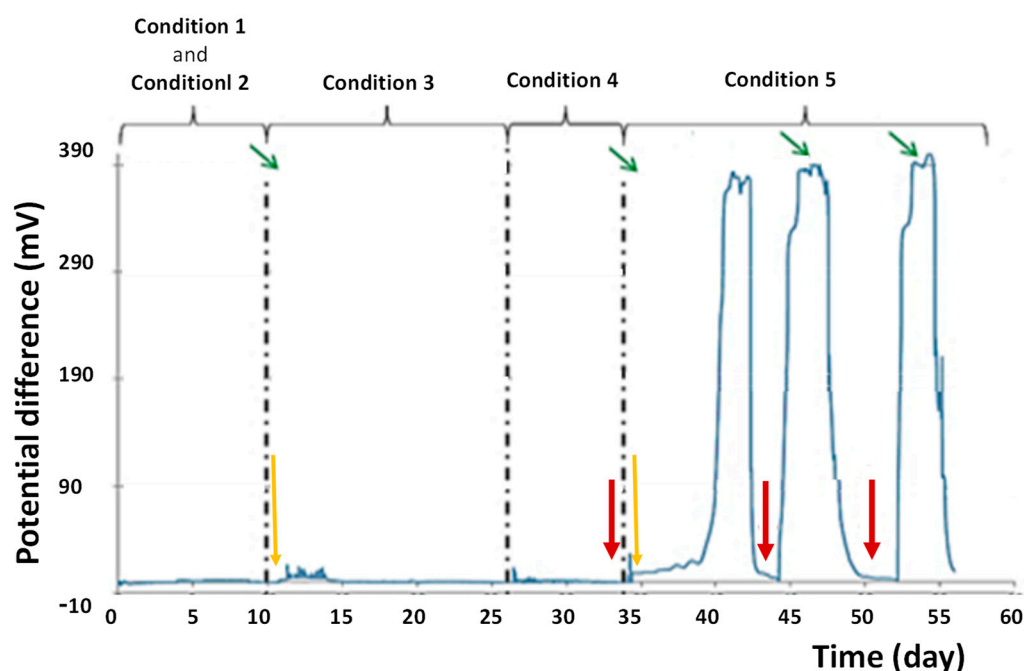


**Figure 2.** Design conditions used to optimize the MFC assembly by measuring potential differences over time without agitation in the anodic compartment. Conditions 1 and 2: copper wire + synthetic effluent + carbon felt (electrode distance of 5 cm to Nafion membrane); Condition 3: addition of biomass inoculum; Condition 4: reduction of electrode distance to 2.5 cm; Condition 5: electrodes pressed against the Nafion membrane. Yellow arrows correspond to biomass inoculum injection, and green and red arrows indicate the beginning and end of each synthetic wastewater effluent feeding cycle.

In the next step, the anodic chamber was inoculated with biomass consortium (Sample ID 4 in Supplementary Materials Table S1), and after about 24 h, a thin biofilm with low uniformity was formed on the electrode surface (Condition 3). A very low voltage of about 10 mV from day 11 to day 15 was detected, probably due to the microbial activity adjustment to the environmental conditions. However, electrical energy production was not detected from day 15 to 25.

The small voltage change detected on day 26 was due to the reduced electrode distance from the Nafion membrane to 2.5 cm (Condition 4), but it was not significant, and stability was lost on day 27.

On day 34, a slight increase in potential difference was observed when the carbon felt electrodes were pressed against the Nafion membrane and adding new biomass inoculum to the anodic compartment (Condition 5). A sharp potential increase was observed on day 39, nearly reading a voltage of 382 mV on day 40, stable for about 2 days (collection of the biofilm sample from anode surface identified as Sample ID 9 in Supplementary Materials Table S1). After that, a sharp decrease in the voltage occurred, achieving almost 0 mV of potential difference at day 44, when 270 mL of exhausted synthetic effluent was discharged. Then, a new biomass inoculum and synthetic wastewater effluent were fed to the anodic compartment initiating a new cycle. Three individual electrical energy production cycles were carried out with a maximum potential difference of 385 mV and stable for about 3 days (Figure 2). A new biofilm sample was collected from the anode surface, identified as Sample ID 10 in Supplementary Materials Table S1.

These design condition experiments allow for optimizing the MFC setup configuration and enhancing performance. When both electrodes were pressed against the Nafion membrane, it facilitated the transport of hydrogen ions, leading to a significant generation of potential differences between the anodic and cathodic electrodes. These results also prove that the dominant ohmic losses in this MFC cell configuration were associated with

ion transportation through the electrolyte (the Nafion membrane). Reducing the path that the hydrogen ions need to travel between the anode and cathode electrodes enhances the MFC performance as the resistance through very conductive materials such as carbon felt and copper wires are neglected [51].

This conclusion also concurs significantly with the results obtained by Deng et al. [52] using a similar MFC design with activated carbon electrodes. This MFC configuration was selected and used for further experiments in this work.

### 3.2. Effect of the External Resistance

The polarization effect on the MFC performance without agitation in the anodic compartment by using different external resistances (20, 220, 560, 820, 1000, 5000  $\Omega$ ) integrated into the external circuit between the anode and cathode electrodes were evaluated (Condition 6). In every test, a new resistance was introduced into the external electric circuit between electrodes, and the measurements were carried out 30 to 60 min after their introduction, as this is the optimal time interval required to reach equilibrium in the internal MFC system.

The maximum potential difference of the MFC was measured in open circuit voltage (OCV), i.e., the maximum voltage that can be obtained in an MFC system with infinite resistance. The voltage measured in the MFC decreased with the reduction in resistance integrated into the external electric circuit (Table 2). The current density (CD) and power density (PD) for each resistance were calculated from the voltage values measured.

**Table 2.** Values obtained (voltage, DC, and DP) for each resistance tested and under OCV.

	External Resistance ( $\Omega$ )						
	OCV	5000	1000	820	560	220	20
Voltage (mV)	498	422	374	272	212	114	8
CD (mA/m <sup>2</sup> )	0	28	125	111	127	174	129
DP (mW/m <sup>2</sup> )	0	12	47	30	27	20	1

The maximum CD (174 mA/m<sup>2</sup>) and DP (47 mW/m<sup>2</sup>) in this MFC configuration were achieved with external resistance of 220 and 1000  $\Omega$ , respectively. However, the maximum DP in this MFC configuration was achieved for 1000  $\Omega$ , a value already used in the previous design condition experiments in this work, and it was identified for other authors as the best value [24,36,53,54]. Therefore, as these studies are performed only in batch operation mode, the resistance of 1000  $\Omega$  integrated into the external electric circuit was selected to evaluate the following design conditions and the MFC performance.

### 3.3. Effect of the Agitation Inside of the Anodic Compartment

The effect of agitation in the bottom of the anodic compartment on the electrical energy generation by the MFC under the abiotic cathode configuration was evaluated. After MFC assembly, the anodic compartment was inoculated with biomass inoculum and fed with the synthetic wastewater effluent, and the content was homogenized by magnetic agitation at the bottom (Condition 7).

During this design condition experiment, after about 5 to 10 days for biomass growth and biofilm formation and covering the carbon felt surface, a unique electrical energy production cycle was observed and stable for about 15 days, reaching a potential difference of about 428 mV (Figure 3).

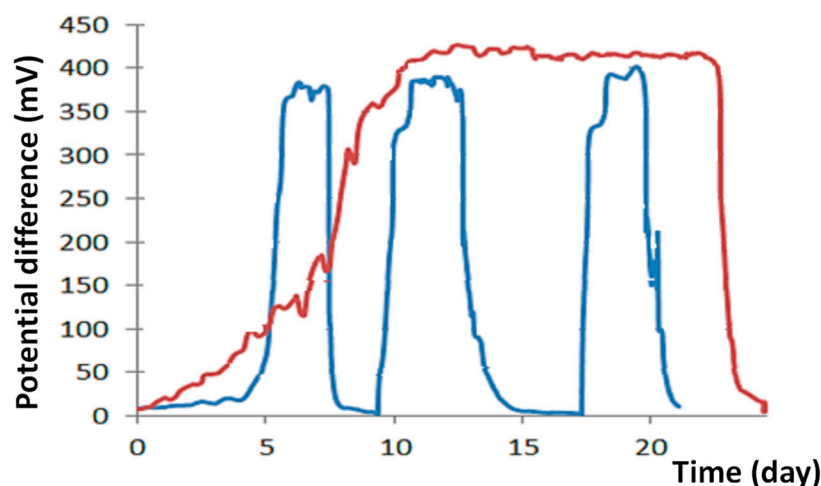


**Figure 3.** Comparison of MFC performance with agitation (Condition 7—red line) and without magnetic agitation (Condition 5—blue line) in the anodic compartment loaded with the synthetic wastewater effluent and under the MFC abiotic cathode configuration.

The agitation inside the anodic compartment led to the homogenization of liquid content and minimized microorganism sedimentation. It also favored the formation of a gradual biofilm on the electrode surface for 7 to 8 days, with an increase in the potential difference being observed. With the saturation of the immobilized microorganisms on the anode electrode surface, the maximum value of the potential difference was 430 mV. Furthermore, a continuous generation of bioenergy occurred, characterized by a unique cycle with an almost constant generation of electric current for 15 days ( $\approx 400$  mV, between days 10 to 25). These results greatly contrast with the three bioenergy production cycles, averaging about 3/4 days, and a voltage of about 385 mV was observed without agitation in the anodic compartment (Condition 5) (Figure 3).

The short cycle observed (3/4 days) without agitation is due to a fast consumption of organic compounds by microorganisms accumulated on the electrode surface but mainly deposited and accumulated in the bottom of the anodic compartment (Condition 5). Consequently, the global generation of electric current was higher with agitation concerning the long cycle of 20 days (Condition 7).

A power density (PD) of  $51 \text{ mW/m}^2$  was calculated for the design condition with agitation (Condition 7) and  $41 \text{ mW/m}^2$  without agitation (Condition 5), i.e., 19% higher. This increase in the electric generation efficiency is lower than that one observed by Pharm et al. [55], who reported that higher high shear stress in the anodic compartment led to a doubling in the thickness of the biofilm on the anode electrode surface and affected bacterial consortium, as the power output was three times higher compared to the low shear stress condition. However, in this work, the agitation in the anodic compartment led to a global electric power generation 85% higher than the global energy production of the three cycles without agitation for 25 days. Despite this, higher operational costs characterize the MFC configuration with agitation in the anodic compartment, and an economic evaluation is advised.

Biofilm samples were collected from the anode surfaces without agitation (Condition 5) and with agitation (Condition 7), identified as sample ID 5 and 6, respectively, in Supplementary Materials Table S1. According to the microbial composition analysis (Section 3.7), the microbial consortium in the anode surface is similar, so the potential difference in both design conditions is about the same ( $\sim 400$  mV).

The wastewater treatment efficiency was not affected for the design condition with agitation (Condition 7) as the COD removal at the end of the cycle of 25 days was almost higher than 87% but was lower than 95% in each cycle obtained for the design condition without agitation (Condition 5). MFC configuration without agitation probably favors the proliferation and accumulation of fermentative bacteria in the bottom of the anodic

compartment. The absence of agitation leads to a faster carbon source consumption and a higher number of cycles, i.e., three versus only one observed with magnetic agitation for about the same period (25 days).

The agitation in the bottom of the anodic compartment was selected and used for further experiments in this work.

### 3.4. Abiotic Cathode with Potassium Permanganate

Oxygen is the most often used oxidant in MFC systems due to its high theoretical redox potential and availability. However, achieving high practical redox potentials requires a catalyst integrated into the cathode electrode (e.g., platinum), which is very expensive and degrades over time. Other oxidant substances studied in MFC systems include ferrocyanide [56] and permanganate [57,58].

The anodic compartment of MFC with abiotic cathode configuration was fed with new synthetic effluent and biomass inoculum. The potential difference increased, achieving about 380 mV after 8 days (Figure 4A). Then, the phosphate buffer in the cathode compartment was supplemented with potassium permanganate (0.4 mM) characterized by a typical red color to check the MFC performance (Figure 4B).

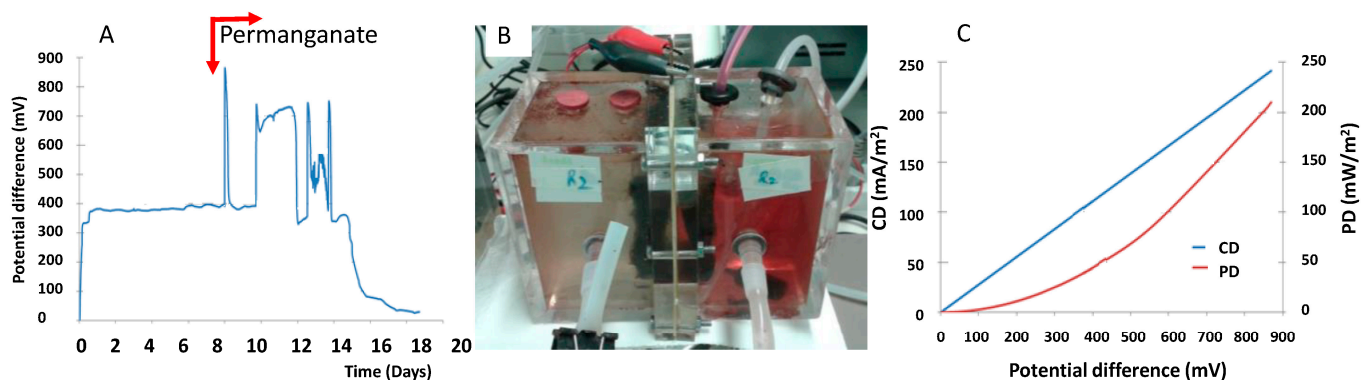


**Figure 4.** Abiotic cathode with potassium permanganate. (A) Voltage vs. time in the MFC abiotic cathode during the first 8 h and then containing potassium permanganate (0.4 mM) in phosphate buffer. (B) The cathode compartment exhibits a typical red color. (C) The polarization curve of the abiotic cathode containing potassium permanganate (0.4 mM) in phosphate buffer. The red arrows state the addition of the permanganate to the cathodic solution.

The voltage was continuously measured, and a unique cycle of electrical energy generation during 19 days was observed (Figure 4A). Initially, about 380 mV was observed in the first 7 days without permanganate. Then, pulses of the potential difference occurred on day 8, between days 10 and 12, and days 13 and 14 due to the reaction of permanganate with hydrogen ions and electrons in the cathodic compartment (Figure 4A). The potential difference increased to 760 mV about 100% compared to the one (380 mV) obtained with the MFC abiotic cathode configuration with only phosphate buffer in the cathodic chamber (Figure 4A).

By day 15, the electrical energy production gradually started to decrease, and a minimum potential difference was achieved on day 18, corresponding to the almost total consumption of the carbon source in the synthetic wastewater effluent contained in the anodic compartment.

The impulse periods of energy generation led to a maximum potential difference in this MFC configuration of 870 mV and OCV of 970 mV. The corresponding PD and CD vs. tension values were 210 mW/m<sup>2</sup> and 242 mA/m<sup>2</sup>, respectively (Figure 4C).

The value of DP obtained in this work is relevant as it is about 157% higher than those obtained by Rahimnejad et al. [58] (133 mW/m<sup>2</sup>) using similar conditions, i.e., in an MFC with an abiotic cathode also containing potassium permanganate. However, Gurav et al. [5] and Lee et al. [59] achieved PD of 2280 mA/m<sup>2</sup> and 17,100 mA/m<sup>2</sup>, respectively,

values higher than those obtained in this work. These both works presented excellent PD values as the cathode is equipped with platinum-coated carbon felt functions as a catalyst of ferricyanate in phosphate buffer used as the oxidant agent in the cathode compartment.

Work performed in this study confirmed that oxygen reduction in the cathodic reaction probably limits the production of electrical energy in the MFC abiotic cathode configuration tested previously, which agrees with the works of other authors [58,60]. Although the enhancement of electrical energy generation encourages using these mediating oxidant agents (e.g., permanganate, ferricyanate, and others), it is necessary to consider prior careful environmental and economic evaluation [51].

### 3.5. Cyclic Voltammetry with Anode Electrode of the MFC Abiotic Cathode Configuration

The electrochemical characterization of the MFC abiotic cathode configuration was assayed in the synthetic wastewater effluent by cyclic voltammetry (CV). Figure 5 shows the multicycles using the anode electrode as the working electrode. The assay starts toward cathodic potentials, reaching a potential of  $-1.0$  V, where the scan direction is inverted toward anodic potentials (maximum  $0.8$  V).

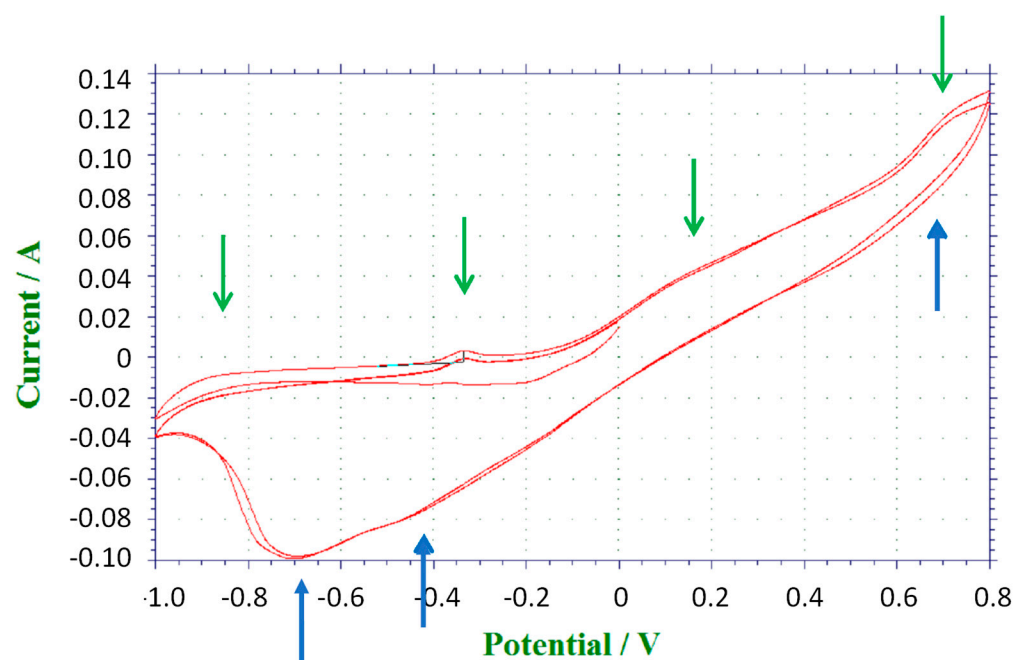


**Figure 5.** CV of the carbon felt electrodes for electrochemical MFC characterization. The anode electrode was used as the working electrode, the abiotic cathode electrode functioned as the counter electrode, and Ag/AgCl was the reference electrode. The green and blue arrows identified the oxidation and reduction peaks, respectively.

The arrows indicate the redox processes occurring, the green arrows identify the oxidation current peaks, and the blue arrows identify the reduction peaks. The results from the first and subsequent cycles show that the carbon felt of the anode surface exhibits several redox processes (Figure 5). The current occurs due to the spontaneous oxidation of some constituents contained in the synthetic wastewater effluent and, eventually, metabolites biosynthesized by the microorganisms immobilized on the carbon felt surface. The reduction processes result from the previous anodic processes.

The CV results confirm the direct redox activity on the anode electrode surface, resulting from the biotic environment on biofilm [54,61]. The oxidation peaks correspond to electron transfer by diverse microbial mechanisms responsible for the direct and indirect transfer of electrons to anode electrodes, in line with previous studies [54,60].



### 3.6. MFC Configurations with the Air-Breathing Cathode in Direct Contact with Air

#### 3.6.1. Carbon Felt Electrode without Any Modification

An MFC air-breathing cathode configuration with the carbon felt without modification (Scheme 1, configuration A) was initially tested as a control. No electric generation occurred, i.e., the potential difference remained at zero for several days (data not shown), and no oxygen reduction happened in this condition, even though a visible biofilm had formed on the anode electrode surface.

Since the carbon felt is hydrophobic, these results suggest that the degree of moisture in the air is not enough to humidify the carbon felt electrode and, probably, insufficient to allow the transport of hydrogen ions from the Nafion membrane to cathode carbon felt that constitutes the air-breathing electrode.

#### 3.6.2. Carbon Felt Electrode Modified with Ion Jelly<sup>®</sup>

The next step was operationalizing MFC configurations with the air-breathing cathode. First, Ion Jelly<sup>®</sup> was deposited on one side of the dry carbon felt and pressed against the Nafion membrane (Scheme 1, configuration B), and secondly, Ion Jelly<sup>®</sup> containing laccase (IJ-Lac) was embedded in previously wetted carbon felt in water for 24 h (Scheme 1, configuration C). Both air-breathing cathode electrodes were assembled in the cathodic compartment in direct contact with air.

#### IJ Deposited on One Top Side of the Carbon Felt and Pressed against the Nafion Membrane

The IL employed to prepare this hydrogel was 1-butyl-3-methylimidazolium dicyanamide [bmim][N(CN)<sub>2</sub>]. This IL was selected since it preserves its shape and gelatinous structure in contact with the air and is not too viscous, thus facilitating its handling [34].

The anodic chamber with the air-breathing cathode modified with IJ (Scheme 1, configuration B) was inoculated with the wastewater treatment sample (Sample ID 3 in Supplementary Materials Table S1). The potential difference rose to approximately 75 mV, achieving a power density of 1.9 mW/m<sup>2</sup> (Figure 6A). During the first 4 days, the power generation remained at that level, which was most likely due to the microbial adaptation and biofilm formation on the carbon felt, i.e., on the anode electrode surface (Figure 6A) [62].

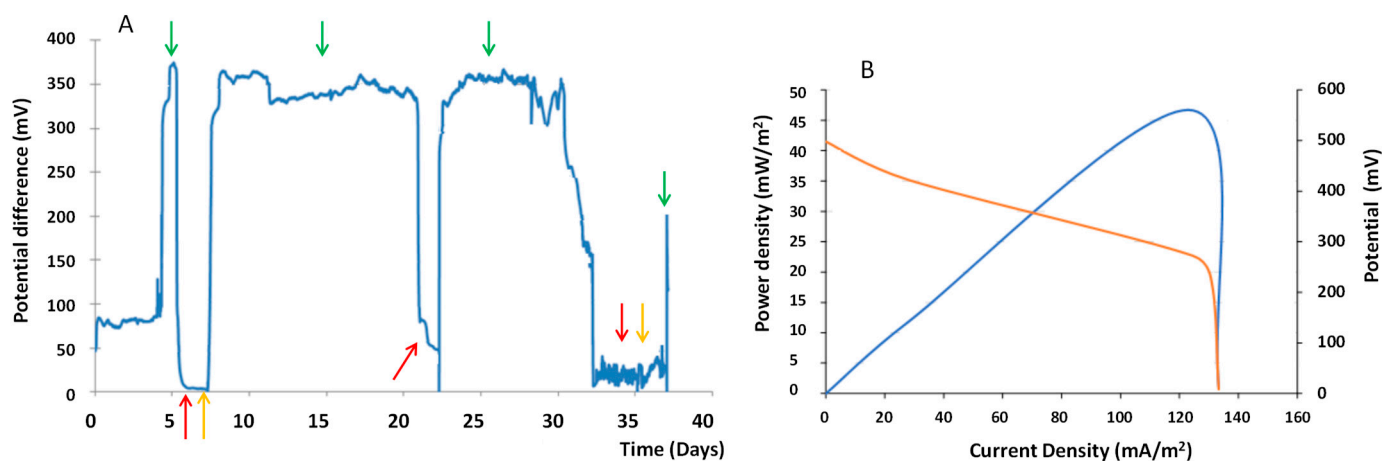


**Figure 6.** Performance of the MFC air-breathing with IJ cathode (Scheme 1, configuration B). (A) Time versus voltage variation where the green and red arrows represent the beginning and end of a cycle, respectively, and the yellow arrows the injection of biomass. (B) Polarization and power curves with the potential difference (blue line) and power density (orange line).

Afterward, the voltage of this MFC air-breathing configuration increased sharply, reaching a maximum voltage of 375 mV. The power production spiked to 39 mW/m<sup>2</sup>, with DC of 104 mA/m<sup>2</sup> and OCP reaching 498 mV, before sharply decreasing before a day had passed (Figure 6A,B). The synthetic effluent addition did not recover power

production, so a new biomass inoculum was added to the anodic chamber. The power generation increased to previously observed levels (~350 mV), and this MFC air-breathing configuration could operate for 14 days at close to 350 mV. When energy production decreased again, adding fresh synthetic effluent restored the power generation for another 8 days of operation. A microbial sample was collected from the anode surface during the third cycle on day 25 (Sample ID 10 in Supplementary Materials Table S1). After this third cycle of bioelectricity generation, the power decreased again. Adding new synthetic effluent and biomass inoculum restored a brief spike at 200 mV for one or two hours and then decreased irreversibly to 0 mV (Figure 6A).

A power density of 48 mW/m<sup>2</sup> and a current density of 130 mA/m<sup>2</sup> were calculated for the performance of the MFC air-breathing with IJ cathode configuration (Scheme 1, configuration B) using a 1 kΩ resistance with OCPs of 534 mV, and the relationship between these variables is represented in Figure 6B. These values are relevant and correspond to about 400% higher than those obtained by Das and Calay [12] using a pure culture of *Shewanella baltica* 20 to inoculate the anodic chamber and promote the formation of a biofilm on the carbon felt electrode surface. Furthermore, the power density obtained in the MFC air-breathing cathode based on carbon felt modification with Ion Jelly<sup>®</sup> is also the same magnitude as that obtained by Merino-Jimenez et al. [21] and Mateo et al. [13] using activated carbon and a microporous catalytic layer of platinum for the oxygen reduction reaction directly from the air.

The performance of this MFC air-breathing with IJ cathode configuration was confirmed and compared to the same MFC setup but operating with biocathode and abiotic cathode configurations (Supplementary Materials Figure S1), achieving similar values reported in a previous work carried out by the authors [36]. There was another similar operational behavior of this MFC air-breathing cathode concerning the biocathode and abiotic cathode, i.e., after a period of stabilization, all of them were able to operate for power generation cycles of about 20 days before fresh synthetic effluent needed feeding again, and in some cases, the addition of new biomass inoculum. However, this MFC air-breathing IJ cathode configuration operated for 30 days but much less than the total operation time of about 195 and 230 days reported for the biocathode and abiotic cathode, respectively (Supplementary Materials Figure S1 and also include the reference [63]).

The lower operability of the MFC air-breathing IJ cathode configuration, i.e., a limited number of power generation cycles, could be related to the stability of the IJ deposited on the carbon felt surface, i.e., the air-breathing cathode electrode. After dismantling the cell, the IJ layer was found to have shrunk slightly and showed signs of moisture loss, rigidity, and much less flexibility than fresh IJ preparation due to prolonged contact with air at room temperature (about 30 days). This phenomenon can probably be minimized using water-saturated air or occasionally wetting the cathode electrode surface.

The MFC air-breathing IJ cathode configuration yielded these results, which is slightly surprising since there is no catalyst to promote oxygen reduction in the cathode [64]. The process and mechanism behind this phenomenon seem not yet clear. There is no knowledge that IJ has the catalytic ability to reduce oxygen. The IJ cathode assay involving oxygen reduction is necessary to clarify and understand these results. However, the other possibility and probably the most plausible hypothesis is due to the increased efficiency of H<sup>+</sup> exchange promoted by the high electroconductivity of the IJ from the Nafion membrane to the surface of the carbon felt electrode. The high hydrogen ion transfers probably significantly decrease the ohmic voltage losses between the Nafion membrane and carbon felt surface in this MFC air-breathing configuration.

#### IJ Containing Laccase and Embedded into the Carbon Felt

The next step was to prepare and test a new carbon felt electrode based on the IJ containing laccase. Laccases are multicopper oxidases that are found in trees or fungi. They have low substrate specificity and catalyze the oxidation of various organic compounds, such as lignin and the phenol compounds that arise from lignin degradation, coupling

this process with oxygen reduction to water [65]. Their T1 copper centers accept electrons and usually possess a high thermodynamic redox potential (+0.72 V vs. NHE for *Trametes versicolor* laccase at pH 5.8) [66]. Some of these properties vary according to the microorganism of origin [67]. Laccases have been used in several MFCs, most notably with mediator electron transfer (MET) in modified Nafion membranes [29,68] or with redox osmium hydrogels [69], creating biocathodes with very high current densities. Direct electron transfer (DET) with laccase has also been investigated using, for example, carbon nanostructures [70–73] or modified films of poly(3,4-ethylene dioxythiophene) [74].

In this work, *Trametes versicolor* laccase was added during the preparation of Ion Jelly using the same methodology used to stabilize oxidoreductase enzymes [34,35]. This experiment employed the laccase to study the possible enhancement of biocatalysis of the oxygen reduction directly from air through this new MFC air-breathing IJ–Lac cathode configuration.

The MFC air-breathing electrode constituted by wetted carbon felt embedded with IJ–Lac (Scheme 1, configuration C) had an adaption period of 2 days until there was a voltage spike to 168 mV (power density of 9 mW/m<sup>2</sup> and OCP of 192 mV), after which voltage decreased and remained in the 10–20 mV range for 10 days (power density of 0.1 mW/m<sup>2</sup>). Adding new microbial suspension generated only a smaller voltage peak, but no considerable and consistent improvement in power generation was observed (Figure 7).

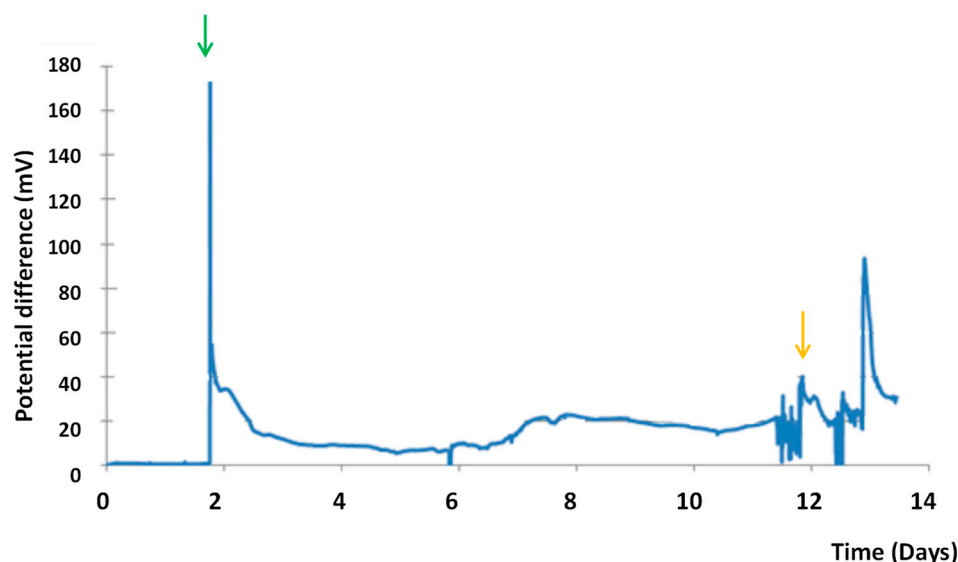


**Figure 7.** Time–voltage on the MFC air-breathing cathode embedded with Ion Jelly containing laccase (IJ–Lac) (Scheme 1, configuration C), where the green arrow represents the start cycle and yellow injecting biomass.

The maturation step allowed the IJ–Lac embedded inside the carbon felt. However, new experiments should be performed to understand better the mechanism of carbon felt modification in these conditions. Furthermore, the presence of the laccase used as catalysts in this MFC air-breathing IJ–Lac cathode promoted directly insignificant oxygen reduction from the air. The lower performance observed with this MFC air-breathing IJ–Lac cathode should be associated with the inefficient catalytic activity of laccase in this condition, probably due to the inactivation of the enzyme or by the low oxygen solubility in the IJ–Lac embedded in wetted carbon felt.

A more careful analysis of both MFC air-breathing configurations results suggests that the performance difference observed is due to the IJ layer position as the IJ–Lac buried inside of carbon felt is not in direct contact with the Nafion membrane. Having an IJ layer on the top side of carbon felt and pressed against the Nafion membrane establishes better contact and transfers the ions (H<sup>+</sup>) more efficiently than having IJ–Lac buried inside the carbon felt. Additionally, the IJ layer on one top side of the carbon felt (Scheme 1,

configuration B) seems the most suitable for MFC air-breathing operation due to its high conductivity associated with IJ between the Nafion membrane and carbon felt cathode electrode.

### 3.7. Analysis of Microbial Consortium

Several factors can influence the performance of MFCs, such as temperature, pH, nature of the substrate and its concentration, reactor design, electrode material, external resistance, and others. Nevertheless, one of the most important is the biomass inoculum source used to start the microbial consortium community in the MFC.

This work used a biomass inoculum collected from the wastewater treatment plant (Chelas, Lisbon city, Portugal). When the anodic chamber was fed with synthetic wastewater effluent, the biofilm grew on the carbon felt surface in the optimized MFC design condition. The microbial communities were analyzed in the inoculum, and the biofilm samples collected from the anode electrode surface, especially when the electric generation by the MFCs was stable (Table 3).

**Table 3.** Identification of the samples collected from the wastewater treatment plant (Chelas, Lisbon, Portugal) and from the biofilms formed on the anode electrode surface of MFCs.

Sample ID	Sample Description
1	As a control
2	As a control
3	Used to inoculate the anodic chambers of MFC air-breathing cathodes (Figures 6 and 7)
4	Used to inoculate the anodic chamber during the design condition number 3 on day 10 (Figure 2)
5	Collected during design condition number 5 on day 40 (Figure 2)
6	Collected during design condition number 5, on day 55 and in the 3rd cycle (Figure 2)
7	Collected during design condition number 7 on day 20 of the unique cycle (Figure 3)
8	Collected after 4/5 cycles on day 80 of electric generation of MFC abiotic cathode (Figure S1)
9	Collected after 4/5 cycles on day 80 of electric generation of MFC biocathode (Figure S1)
10	Collected after the 3rd cycle on day 25 of electric generation of MFC air-breathing cathode modified with IL (Figure 6)

After sequencing and OTU taxonomy assignment, variable numbers of distinct OTUs were found in the samples analyzed. However, the total number of reads was higher in samples from MFC reactors 1 and 2 than in the samples collected from the wastewater treatment plant (sample ID 1 to 4). The total numbers of distinct OTUs were lower in the MFC reactors than in the samples collected from the wastewater treatment plant (Table 4). This lower number of OTUs is reflected by the lower Shannon index (a measure of microbial diversity) found for biofilm samples from reactors compared to the one from wastewater treatment and control (Table 4).

**Table 4.** Total reads, OTUs, and diversity index (Shannon index) for samples from reactors 1 and 2 (samples 5–10), wastewater treatment (samples 3, 4), and control samples (samples 1, 2).

Sample #	Total Reads	Total OTUs	Shannon Index
1	35,299	1074	5.8
2	36,902	1089	5.8
3	36,260	815	4.7
4	39,148	821	4.8
5	42,230	229	3.1
6	45,334	240	3.2
7	36,266	250	3.0
8	38,516	236	3.6
9	29,917	423	3.9
10	33,711	178	2.8

Although the sequencing results did not allow the identification of the bacterial community at the species level, various OTUs belonging to taxa known to be exoelectrogenic were identified in the MFC reactors. This difference is the case of OTUs 323, 695, 1173, 1105, 1301, and 2260, which belong to the Desulfuromonadales order to which the well-known electrogenic *Geobacter* spp. also belongs. These results confirm the presence of Geobacteracea, one of the most common bacteria in the microbial consortium in MFC systems [75,76].

OTUs 203 410, 599, and 1034, belonging to the *Rhodoferax* genus, and OTU 995, related to the *Pseudomonas* genus, were identified among the microbial communities inside MFC reactors (Table 4). These two genera also contain electrogenic species. No OTUs related to the genus *Aeromonas* or *Shewanella*, also known to contain electrogenic species, were detected in the MFC reactors.

OTUs 806 and 2161, related to the *Enterococcus* genus known to play a role as indirect electrogenic bacteria, were found exclusively in the wastewater treatment samples used to inoculate the MFC reactors and were not detected among the microbial populations inside the reactors (Table 4).

Table 5 summarizes the 25 most abundant bacterial genera across all samples and includes information on each bacteria from the MiDAS database. The novel phylotype *Candidatus Amarilinum* is second-most abundant and especially abundant in the wastewater treatment samples (samples 3 and 4 are highly similar), whereas control samples (1 and 2) bacteria are slightly more diverse but with lower abundance.

The most abundant bacteria in the MFC anodic chambers belong to the chemoorganotroph *Rhodococcus* genus and the Rhodocyclaceae unclassified OTU\_6. These two bacteria genera are abundant in most samples except those collected in the wastewater treatment plant (samples 1, 2, 3, and 4), as they were not significantly detected in these samples. This accumulation and abundance of the *Rhodococcus* genus in the MFC anodic chambers are due to the selection and concentration of the bacteria after several cycles of COD reduction and electric generation.

Samples 5, 7, and 8 shared many of the same bacteria genera, although in different abundances. The highly abundant *Rhodococcus* dominates sample 5, whereas sample 7 has the suggested GAO *Propionivibrio* and the unclassified OTU\_6 in almost equally high abundance. Sample 8 has *Rhodococcus* as the most abundant organism, but not as predominant as in sample 5.

Samples 6, 9, and 10 presented similar communities, although each sample has some abundant genera not found in the other two samples. The most abundant genus in sample 6 is *Azospira*, which is found in low abundance in the other samples.





Samples 7, 8, 9, and 10 collected from the R1 and R2 MFC reactors show a similar bacterial composition. Most genera are shared across all four samples in varying abundances, although some differences are noteworthy. OTU\_6 is highly abundant in samples 7 and 10 but low in samples 8 and 9. *Propionivibrio* is the most abundant genus in sample 7, while found in lower abundance in the other samples.

Multivariate statistics (PCA) was used to compare the overall microbial composition of all samples (Figure 8). Three main clusters were observed. Samples 1 and 2, along with samples 3 and 4, form two distinct groups. Sample 9 is similar to the remaining biofilm samples but is not part of the close group they formed (samples 5, 6, 7, 8, 10). Distance between the sample dots signifies similarity: the closer the samples plot, the more similar microbial composition they have (Figure 8).

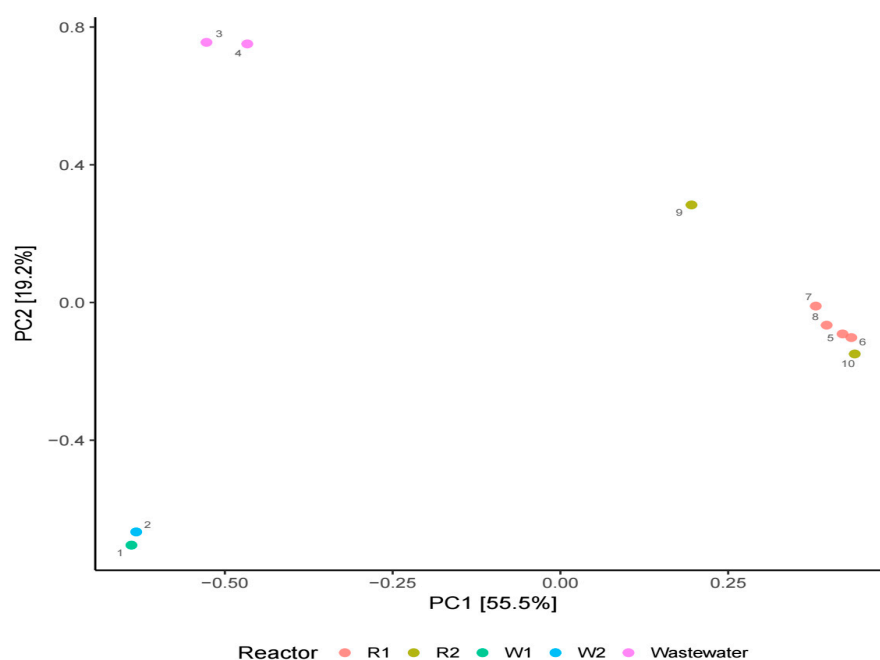


**Figure 8.** Principal component analysis (bacteria). Identification of samples with similar microbial communities using multivariate statistics (PCA). Each point represents the microbial community in a specific sample. The sample numbers between 1 and 10 are according to the identification in the Table 3.

#### 4. Conclusions

Different types of cathodes, namely abiotic cathode, biocathode, and air-breathing cathodes, demonstrated capacity in treating a synthetic wastewater effluent based on acetate as the primary carbon source and bioelectricity generation. The operational stability of the abiotic and biocathode, however, was longer than the one observed for the MFC air-breathing configuration.

The different MFC configurations show similar performance in terms of CD, PD, potential difference, COD reduction, and coulombic efficiency due to the high similarity of the microbial consortium assayed in the biofilm collected from the anode electrode surface.

The configuration of Ion Jelly<sup>®</sup> deposited as a thin layer on one top side of the dry carbon felt, pressed against, and in deep contact with the Nafion membrane shows a promising opportunity in designing MFC air-breathing cathodes. According to our expertise, this conclusion is due to the excellent Ion Jelly<sup>®</sup> electroconductivity properties that can be designed before modifying the carbon felt electrode, significantly improving the MFC air-breathing cathode performance.

Potassium permanganate (0.4 mM) in the abiotic cathode compartment increases 100% the potential difference concerning phosphate buffer alone. The experiment with the

permanganate suggests that the oxygen reduction in the cathode electrode can be a limited stage in MFC abiotic cathode configuration performance.

The samples collected from biofilm anodic electrodes of the MFCs presented a lower microbial diversity than the wastewater treatment used as inocula and control samples. This microbial difference is due to the fewer bacterial species adapted to the highly selective niches constituted by MFC systems.

**Supplementary Materials:** The following supporting information can be downloaded at <https://www.mdpi.com/article/10.3390/en16104238/s1>: description of DNA extraction, sequencing, and sequence data analysis, Operational stability and performance MFC abiotic cathode and biocathode configurations, and COD reduction efficiencies. Table S1: The microbial composition of the samples collected from the wastewater treatment plant streams (Chelas, Lisbon city, Portugal) and the biofilm on the carbon felt surface of MFC anodic reactors (R1 and R2). Figure S1: The potential difference over time. (A) MFC with abiotic cathode configuration. (B) for MFC biocathode configuration. The green and red arrows represent the beginning and end of each cycle, the yellow arrows correspond to biomass inoculum injection, and the orange arrow identifies an academic pause. The Supplementary Materials also named the references between [39–48] and [63].

**Author Contributions:** Conceptualization, R.N.L.C. and L.P.F.; investigation, R.N.L.C. and S.V.R.; methodology, S.A.S., J.H.L., and C.M.C.; formal analysis, J.H.L. and S.A.S.; project administration, L.P.F.; supervision, C.M.C., J.H.L., and L.P.F.; writing—original draft, L.L.M.; writing—review and editing, C.M.C., J.H.L., and L.P.F. All authors have read and agreed to the published version of the manuscript.

**Funding:** This research was funded by Fundação para a Ciência e a Tecnologia projects DSAIPA/DS/0117/2020, UIDB/04565/2020, and UIDP/04565/2020, by the Associate Laboratory Institute for Health and Bioeconomy—i4HB project LA/P/0140/2020. This work was supported by the Associate Laboratory for Green Chemistry—LAQV financed by national funds from FCT/MCTES (UIDB/50006/2020). We also thank Fundação para a Ciência e Tecnologia (FCT) for funding (SFRH/BD/77568/2011 (R.N.L.C.); SFRH/BPD/80293/2011 (R.M.A.)). C.M.C. acknowledges FCT for the Ciência 2008 Program; S.V.R. acknowledges the financial support from FCT (Portuguese Foundation for Science and Technology) for a postdoctoral research grant (FRH/BPD/33864/2009). This work was supported by the Associate Laboratory for Green Chemistry—LAQV, financed by national funds from FCT/MCTES (UIDB/50006/2020 and UIDP/50006/2020); the Institute for Bioengineering and Biosciences—iBB, financed by FCT (UID/BIO/04565/2013); and from Programa Operacional Regional de Lisboa 2020 (Project N. 007317).

**Data Availability Statement:** Not applicable.

**Acknowledgments:** The authors also thank Hélder Leandro da Silva Teixeira for technical support.

**Conflicts of Interest:** The authors declare no conflict of interest.

## References

1. Agenda for Sustainable Development UN 2030. Available online: <https://www.un.org/sustainabledevelopment/development-agenda/> (accessed on 2 April 2023).
2. Bell, K.Y.; Abel, S. Optimization of WWTP aeration process upgrades for energy efficiency. *Water Pract. Technol.* **2011**, *6*, 2. [[CrossRef](#)]
3. Quek, A.; Balasubramanian, R. Life cycle assessment of energy and energy carriers from waste matter—A review. *J. Clean. Product.* **2014**, *79*, 18–31. [[CrossRef](#)]
4. Trapero, J.R.; Horcajada, L.; Linares, J.J.; Lobato, J. Is Microbial Fuel Cell Technology Ready? An Economic Answer towards Industrial Commercialization. *Appl. Energy* **2017**, *185*, 698–707. [[CrossRef](#)]
5. Gurav, R.; Bhatia, S.K.; Choi, T.-R.; Kim, H.-J.; Lee, H.-J.; Cho, J.-Y.; Ham, S.; Suh, M.-J.; Kim, S.-H.; Kim, S.-K.; et al. Seafood Processing Chitin Waste for Electricity Generation in a Microbial Fuel Cell Using Halotolerant Catalyst *Oceanisphaera arctica* YHY1. *Sustainability* **2021**, *13*, 8508. [[CrossRef](#)]
6. Lovley, D.R. Microbial fuel cells: Novel microbial physiologies and engineering approaches. *Curr. Opin. Biotechnol.* **2006**, *17*, 327–332. [[CrossRef](#)]
7. Aiyer, K.S. How Does Electron Transfer Occur in Microbial Fuel Cells? *World J. Microbiol. Biotechnol.* **2020**, *36*, 19. [[CrossRef](#)] [[PubMed](#)]

8. Rahmani, A.R.; Navidjoui, N.; Rahimnejad, M.; Alizadeh, S.; Reza Samarghandi, M.; Nematollahi, D. Effect of different concentrations of substrate in microbial fuel cells toward bioenergy recovery and simultaneous wastewater treatment. *Environ. Technol.* **2020**, *43*, 1–9. [[CrossRef](#)]
9. Das, S.; Ghangrekar, M.M. Tungsten oxide as electrocatalyst for improved power generation and wastewater treatment in microbial fuel cell. *Environ. Technol.* **2020**, *41*, 2546–2553. [[CrossRef](#)]
10. Zhang, X.; Cheng, S.; Liang, P.; Huang, X.; Logan, B.E. Scalable air cathode microbial fuel cells using glass fiber separators, plastic mesh supporters, and graphite fiber brush anodes. *Bioresour. Technol.* **2011**, *102*, 372–375. [[CrossRef](#)]
11. Logan, B.E.; Hamelers, B.; Rozendal, R.; Schroder, U.; Keller, J.; Freguia, S.; Aelterman, P.; Verstraete, W.; Rabaey, K. Microbial fuel cells: Methodology and technology. *Environ. Sci. Technol.* **2006**, *40*, 5181–5192. [[CrossRef](#)]
12. Das, S.; Calay, R.K. Experimental Study of Power Generation and COD Removal Efficiency by Air Cathode Microbial Fuel Cell Using *Shewanella baltica* 20. *Energies* **2022**, *15*, 4152. [[CrossRef](#)]
13. Mateo, S.; Rodrigo, M.; Fonseca, L.P.; Cañizares, P.; Fernandez-Morales, F.J. Oxygen Availability Effect on the Performance of Air-Breathing Cathode Microbial Fuel Cell. *Biotechnol. Prog.* **2015**, *31*, 900–907. [[CrossRef](#)] [[PubMed](#)]
14. Logan, B.E.; Regan, J.M. Microbial fuel cells—Challenges and applications. *Environ. Sci. Technol.* **2006**, *40*, 5172–5180. [[CrossRef](#)] [[PubMed](#)]
15. Logan, B.E. Scaling up microbial fuel cells and other bioelectrochemical systems. *Appl. Microbiol. Biotechnol.* **2010**, *85*, 1665–1671. [[CrossRef](#)]
16. Palmore, G.T.R.; Kim, H.H. Electro-enzymatic reduction of dioxygen to water in the cathode compartment of a biofuel cell. *J. Electroanal. Chem.* **1999**, *464*, 110–117. [[CrossRef](#)]
17. Xu, F.; Kulys, J.J.; Duke, K.; Li, K.; Krikstopaitis, K.; Deussen, H.-J.W.; Abbate, E.; Galinyte, V.; Schneider, P. Redox Chemistry in Laccase-Catalyzed Oxidation of N-Hydroxy Compounds. *Appl. Environ.* **2000**, *66*, 2052–2056. [[CrossRef](#)]
18. Qian, Q.; Su, L.; Yu, P.; Cheng, H.J.; Lin, Y.Q.; Jin, X.Y.; Mao, L.Q. Ionic Liquid-Assisted Preparation of Laccase-Based Biocathodes with Improved Biocompatibility. *J. Phys. Chem. B* **2012**, *116*, 5185–5191. [[CrossRef](#)]
19. Di Lorenzo, M.; Thomson, A.R.; Schneider, K.; Cameron, P.J.; Ieropoulos, I. A small-scale air-cathode microbial fuel cell for on-line monitoring of water quality. *Biosens. Bioelectron.* **2014**, *62*, 182–188. [[CrossRef](#)]
20. Wang, Z.; Mahadevan, G.D.; Wu, Y.; Zhao, F. Progress of air-breathing cathode in microbial fuel cells. *J. Power Sources* **2017**, *356*, 245–255. [[CrossRef](#)]
21. Merino-Jimenez, I.; Santoro, C.; Rojas-Carbonell, S.; Greenman, J.; Ieropoulos, I.; Atanassov, P. Carbon-Based Air-Breathing Cathodes for Microbial Fuel Cells. *Catalysts* **2016**, *6*, 127. [[CrossRef](#)]
22. Kodali, M.; Santoro, C.; Serova, A.; Kabira, S.; Artyushkova, K.; Matanovica, I.; Atanassova, P. Air Breathing Cathodes for Microbial Fuel Cell using Mn-, Fe-, Co- and Ni-containing Platinum Group Metal-free Catalysts. *Electrochim. Acta* **2017**, *231*, 115–124. [[CrossRef](#)] [[PubMed](#)]
23. Tharali, A.D.; Sain, N.; Osborne, W.J. Microbial fuel cells in bioelectricity production. *Front. Life Sci.* **2016**, *9*, 252–266.
24. Liu, H.; Ramnarayanan, R.; Logan, B.E. Production of electricity during wastewater treatment using a single chamber microbial fuel cell. *Environ. Sci. Technol.* **2004**, *38*, 2281–2285. [[CrossRef](#)] [[PubMed](#)]
25. Liu, H.; Logan, B.E. Electricity generation using an air-cathode single chamber microbial fuel cell in the presence and absence of a proton exchange membrane. *Environ. Sci. Technol.* **2004**, *38*, 4040–4046. [[CrossRef](#)]
26. Gupta, G.; Lau, C.; Branch, B.; Rajendran, V.; Ivnitski, D.; Atanassov, P. Direct bio-electrocatalysis by multi-copper oxidases: Gas-diffusion laccase-catalyzed cathodes for biofuel cells. *Electrochim. Acta* **2011**, *56*, 10767–10771. [[CrossRef](#)]
27. Ciniciato, G.P.M.K.; Lau, C.; Cochrane, A.; Sibbett, S.S.; Gonzalez, E.R.; Atanassov, P. Development of paper based electrodes: From air-breathing to paintable enzymatic cathodes. *Electrochim. Acta* **2012**, *82*, 208–213. [[CrossRef](#)]
28. Zloczewska, A.; Jönsson-Niedziolka, M. Efficient air-breathing biocathodes for zinc/oxygen batteries. *J. Power Sources* **2013**, *228*, 104–111. [[CrossRef](#)]
29. Gellert, W.; Schumacher, J.; Kesmez, M.; Le, D.; Minter, S.D. High current density air-breathing laccase biocathode. *J. Electrochem. Soc.* **2010**, *157*, B557–B562. [[CrossRef](#)]
30. Rincón, R.A.; Lau, C.; Luckarift, H.R.; Garcia, K.E.; Adkins, E.; Johnson, G.R.; Atanassov, P. Enzymatic fuel cells: Integrating flow-through anode and air-breathing cathode into a membrane-less biofuel cell design. *Biosens. Bioelectron.* **2011**, *27*, 132–136. [[CrossRef](#)]
31. Lalaoui, N.; de Poulpique, A.; Haddad, R.; Le Goff, A.; Holzinger, M.; Gounel, S.; Mermoux, M.; Infossi, P.; Mano, N.; Lojou, E.; et al. A membrane-less air-breathing hydrogen biofuel cell based on direct wiring of thermostable enzymes on carbon nanotube electrodes. *Chem. Commun.* **2015**, *51*, 7447–7450. [[CrossRef](#)]
32. Higgins, S.R.; Lau, C.; Atanassov, P.; Minter, S.D.; Cooney, M.J. Hybrid Biofuel Cell: Microbial Fuel Cell with an Enzymatic Air-Breathing Cathode. *ACS Catal.* **2011**, *1*, 994–997. [[CrossRef](#)]
33. Vidinha, P.; Lourenço, N.M.T.; Pinheiro, C.; Brás, A.R.T.; Carvalho, T.; Silva, S.; Mukhopadhyay, A.; Romão, M.J.; Parola, J.; Dionisio, M.; et al. Ion-Jelly: A tailor-made conducting material for smart electrochemical devices. *Chem. Commun.* **2008**, *44*, 5842–5844. [[CrossRef](#)] [[PubMed](#)]
34. Carvalho, R.N.L.; Lourenço, N.M.T.; Vidinha Gomes, P.M.; Fonseca, L.J.P. Swelling behavior of gelatin-ionic liquid functional polymers. *J. Polym. Sci. Part B Polym. Phys.* **2013**, *51*, 817–825. [[CrossRef](#)]

35. Lourenço, N.M.T.; Österreicher, J.; Vidinha Gomes, P.; Barreiros, S.; Afonso, C.A.M.; Cabral, J.M.S.; Fonseca, L.P. Effect of gelatin–ionic liquid functional polymers on glucose oxidase and horseradish peroxidase kinetics. *React. Funct. Polym.* **2011**, *71*, 489–495. [CrossRef]
36. Ramanaiah, S.V.; Cordas, C.M.; Matias, S.C.; Venkateswar Reddy, M.; Leitão, J.H.; Fonseca, L.P. Bioelectricity generation using long-term operated biocathode: RFLP based microbial diversity analysis. *Biotechnology* **2021**, *32*, e00693. [CrossRef]
37. Liu, H.; Cheng, S.; Logan, B.E. Production of Electricity from Acetate or Butyrate Using a Single-Chamber Microbial Fuel Cell. *Environ. Sci. Technol.* **2005**, *39*, 658–662. [CrossRef]
38. Torres, C.I.; Kato Marcus, A.; Rittmann, B.E. Kinetics of Consumption of Fermentation Products by Anode-Respiring Bacteria. *Appl. Microbiol. Biotechnol.* **2007**, *77*, 689–697. [CrossRef]
39. Caporaso, J.G.; Lauber, C.L.; Walters, W.A.; Berg-Lyons, D.; Huntley, J.; Fierer, N.; Owens, S.M.; Betley, J.; Fraser, L.; Bauer, M.; et al. Ultra-high-throughput microbial community analysis on the Illumina HiSeq and MiSeq platforms. *ISME J.* **2012**, *6*, 1621–1624. [CrossRef]
40. Ward Jumpstart Consortium Human Microbiome Project Data Generation Working Group. Evaluation of 16S rDNA-based community profiling for human microbiome research. *PLoS ONE* **2012**, *7*, e39315.
41. Bolger, A.M.; Lohse, M.; Usadel, B. Trimmomatic: A flexible trimmer for Illumina sequence data. *Bioinformatics* **2014**, *30*, 2114–2120. [CrossRef]
42. Magoč, T.; Salzberg, S.L. FLASH: Fast length adjustment of short reads to improve genome assemblies. *Bioinformatics* **2011**, *27*, 2957–2963. [CrossRef] [PubMed]
43. Edgar, R.C. UPARSE: Highly accurate OTU sequences from microbial amplicon reads. *Nat. Methods* **2013**, *10*, 996–998. [CrossRef] [PubMed]
44. Wang, Q.; Garrity, G.M.; Tiedje, J.M.; Cole, J.R. Naive Bayesian classifier for rapid assignment of rRNA sequences into the new bacterial taxonomy. *Appl. Environ.* **2007**, *73*, 5261–5267. [CrossRef] [PubMed]
45. Caporaso, J.G.; Kuczynski, J.; Stombaugh, J.; Bittinger, K.; Bushman, F.D.; Costello, E.K.; Fierer, N.; Peña, A.G.; Goodrich, J.K.; Gordon, J.L.; et al. QIIME allows analysis of high-throughput community sequencing data. *Nat. Methods* **2010**, *7*, 335–336. [CrossRef] [PubMed]
46. McIlroy, S.J.; Saunders, A.M.; Albertsen, M.; Nierychlo, M.; McIlroy, B.; Hansen, A.A.; Karst, S.M.; Nielsen, J.L.; Nielsen, P.H. MiDAS: The field guide to the microbes of activated sludge. *J. Biol. Databases Curation* **2015**, *2015*, bav062. [CrossRef] [PubMed]
47. R Core Team R: A Language and Environment for Statistical Computing. 2017. Available online: <https://www.semanticscholar.org/paper/R%3A-A-language-and-environment-for-statistical-Team/659408b243cec55de8d0a3bc51b81173007aa89b> (accessed on 2 April 2023).
48. Albertsen, M.; Karst, S.M.; Ziegler, A.S.; Kirkegaard, R.H.; Nielsen, P.H. Back to Basics—The Influence of DNA Extraction and Primer Choice on Phylogenetic Analysis of Activated Sludge Communities. *PLoS ONE* **2015**, *10*, e0132783. [CrossRef] [PubMed]
49. Carvalho, R.N.L.; Almeida, R.M.; Moura, J.J.G.; Lourenço, N.T.; Fonseca, L.J.P.; Cordas, C.M. Sandwich-Type Enzymatic Fuel Cell Based on a New Electro-Conductive Material–Ion Jelly. *ChemistrySelect* **2016**, *1*, 6546–6552. [CrossRef]
50. American Public Health Association EADAWWAWEF. *Standard Methods for the Examination of Water and Wastewater*; APHA-AWWA-WEF: Washington, DC, USA, 2005.
51. Sun, G.; Thygesen, A.; Ale, M.T.; Mensah, M.; Poulsen, F.W.; Meyer, A.S. The significance of the initiation process parameters and reactor design for maximizing the efficiency of microbial fuel cells. *Appl. Microbiol. Biotechnol.* **2014**, *98*, 2415–2427. [CrossRef]
52. Deng, Q.; Li, X.; Zuo, J.; Ling, A.; Logan, B. Power generation using an activated carbon fiber felt cathode in an up-flow microbial fuel cell. *J. Power Sources* **2010**, *195*, 1130–1135. [CrossRef]
53. Logan, B.E. Exoelectrogenic bacteria that power microbial fuel cells. *Nat. Rev. Microbiol.* **2009**, *7*, 375–381. [CrossRef]
54. Ramanaiah, S.V.; Cordas, C.M.; Matias, S.; Fonseca, L.P. In Situ Electrochemical Characterization of a Microbial Fuel Cell Biocathode Running on Wastewater. *Catalysts* **2021**, *11*, 839. [CrossRef]
55. Pham, H.T.; Boon, N.; Aelterman, P.; Clauwaert, P.; de Schampelaire, L.; van Oostveldt, P.; Verbeken, K.; Rabaey, K.; Verstraete, W. High shear enrichment improves the performance of the anodophilic microbial consortium in a microbial fuel cell. *Microb. Biotechnol.* **2008**, *1*, 487–496. [CrossRef] [PubMed]
56. Rabaey, K.; Verstraete, W. Microbial fuel cells: Novel biotechnology for energy generation. *Trends Biotechnol.* **2005**, *23*, 291–298. [CrossRef] [PubMed]
57. You, S.; Zhao, Q.; Zhang, J.; Jiang, J.; Zhao, S. A microbial fuel cell using permanganate as the cathodic electron acceptor. *J. Power Sources* **2006**, *162*, 1409–1415. [CrossRef]
58. Rahimnejad, M.; Ghoreyshi, A.A.; Najafpour, G.; Jafary, T. Power generation from organic substrate in batch and continuous flow microbial fuel cell operations. *Appl. Energy* **2011**, *88*, 3999–4004. [CrossRef]
59. Lee, S.M.; Lee, H.-J.; Kim, S.H.; Suh, M.J.; Cho, J.Y.; Ham, S.; Song, H.-S.; Bhatia, S.K.; Gurav, R.; Jeon, J.-M.; et al. Engineering of *Shewanella marisflavi* BBL25 for biomass-based polyhydroxybutyrate production and evaluation of its performance in electricity production. *Int. J. Biol. Macromol.* **2021**, *183*, 1669–1675. [CrossRef]
60. Logan, B.E. *Microbial Fuel Cells*, 1st ed.; John Wiley & Sons, Inc.: Hoboken, NJ, USA, 2008; ISBN 978-0-470-23948-3.
61. Massaglia, G.; Fiorello, I.; Sacco, A.; Margaria, V.; Pirri, C.F.; Quaglio, M. Biohybrid Cathode in Single Chamber Microbial Fuel Cell. *Nanomate* **2019**, *9*, 36. [CrossRef]



62. Min, B.; Cheng, S.; Logan, B.E. Electricity generation using membrane and salt bridge microbial fuel cells. *Water Res.* **2005**, *39*, 1675–1686. [[CrossRef](#)]
63. Zhang, G.Y.; Zhang, H.; Zhang, C.; Zhang, G.; Yang, F.; Yuan, G.; Gao, F. Simultaneous nitrogen and carbon removal in a single chamber microbial fuel cell with a rotating biocathode. *Process Biochem.* **2013**, *48*, 893–900. [[CrossRef](#)]
64. Osman, M.H.; Shah, A.A.; Walsh, F.C. Recent progress and continuing challenges in bio-fuel cells. Part II: Microbial. *Biosens. Bioelectron.* **2010**, *26*, 953–963. [[CrossRef](#)]
65. Thurston, C.F. The structure and function of fungal laccases. *Microbiology* **1994**, *140*, 19–26. [[CrossRef](#)]
66. Ivnitski, D.M.; Khripin, C.; Luckarift, H.R.; Johnson, G.R.; Atanassov, P. Surface characterization and direct bioelectrocatalysis of multicopper oxidases. *Electrochim. Acta* **2010**, *55*, 7385–7393. [[CrossRef](#)]
67. Shleev, S.; Jarosz-Wilkolazka, A.; Khalunina, A.; Morozova, O.; Yaropolov, A.; Ruzgas, T.; Gorton, L. Direct electron transfer reactions of laccases from different origins on carbon electrodes. *Bioelectrochemistry* **2005**, *67*, 115–124. [[CrossRef](#)]
68. Heller, A. Electron-conducting redox hydrogels: Design, characteristics and synthesis. *Curr. Opin. Chem. Biol.* **2006**, *10*, 664–672. [[CrossRef](#)] [[PubMed](#)]
69. Soukharev, V.; Mano, N.; Heller, A. A four-electron O<sub>2</sub>-electroreduction biocatalyst superior to platinum and a biofuel cell operating at 0.88 V. *J. Am. Chem. Soc.* **2004**, *126*, 27. [[CrossRef](#)] [[PubMed](#)]
70. Zebda, A.; Gondran, C.; Le Goff, A.; Michael, H.; Cinquin, P.; Cosnier, S. Mediatorless high-power glucose biofuel cells based on compressed carbon nanotube-enzyme electrodes. *Nat. Commun.* **2010**, *2*, 370. [[CrossRef](#)]
71. Miyake, T.; Yoshino, S.; Yamada, T.; Hata, K.; Nishizawa, M. Self-Regulating Enzyme–Nanotube Ensemble Films and Their Application as Flexible Electrodes for Biofuel Cells. *J. Am. Chem. Soc.* **2011**, *133*, 5129–5134. [[CrossRef](#)] [[PubMed](#)]
72. Giroud, F.; Minter, S.D. Anthracene-modified pyrenes immobilized on carbon nanotubes for direct electroreduction of O<sub>2</sub> by laccase. *Electrochem. Commun.* **2013**, *34*, 157–160. [[CrossRef](#)]
73. Minson, M.; Meredith, M.T.; Shrier, A.; Giroud, F.; Hickey, D.; Glatzhofer, D.T.; Minter, S.D. High Performance Glucose/O<sub>2</sub> Biofuel Cell: Effect of Utilizing Purified Laccase with Anthracene-Modified Multi-Walled Carbon Nanotubes. *J. Electrochem.* **2012**, *159*, G166–G170. [[CrossRef](#)]
74. Wang, X.; Latonen, R.M.; Sjooberg-Eerola, P.; Eriksson, J.E.; Bobacka, J.; Boer, H.; Bergelin, M. Direct Electron Transfer of *Trametes hirsuta* Laccase in a Dual-Layer Architecture of Poly(3,4-ethylenedioxythiophene) Films. *J. Phys. Chem. C* **2011**, *115*, 5919–5929. [[CrossRef](#)]
75. Cao, Y.; Mu, H.; Liu, W.; Zhang, R.; Guo, J.; Xian, M.; Liu, H. Electricigens in the anode of microbial fuel cells: Pure cultures versus mixed communities. *Microb. Cell Fact.* **2019**, *18*, 39. [[CrossRef](#)] [[PubMed](#)]
76. Mekuto, L.; Ayomide, V.A.; Olowolafe Pandit, S.; Dyantyi, N.; Nomngongo, P.; Huberts, R. Microalgae as a biocathode and feedstock in anode chamber for a self sustainable microbial fuel cell technology: A review. *S. Afr. J. Chem. Eng.* **2020**, *31*, 7–16. [[CrossRef](#)]

**Disclaimer/Publisher’s Note:** The statements, opinions and data contained in all publications are solely those of the individual author(s) and contributor(s) and not of MDPI and/or the editor(s). MDPI and/or the editor(s) disclaim responsibility for any injury to people or property resulting from any ideas, methods, instructions or products referred to in the content.